

## COMMUNICATION

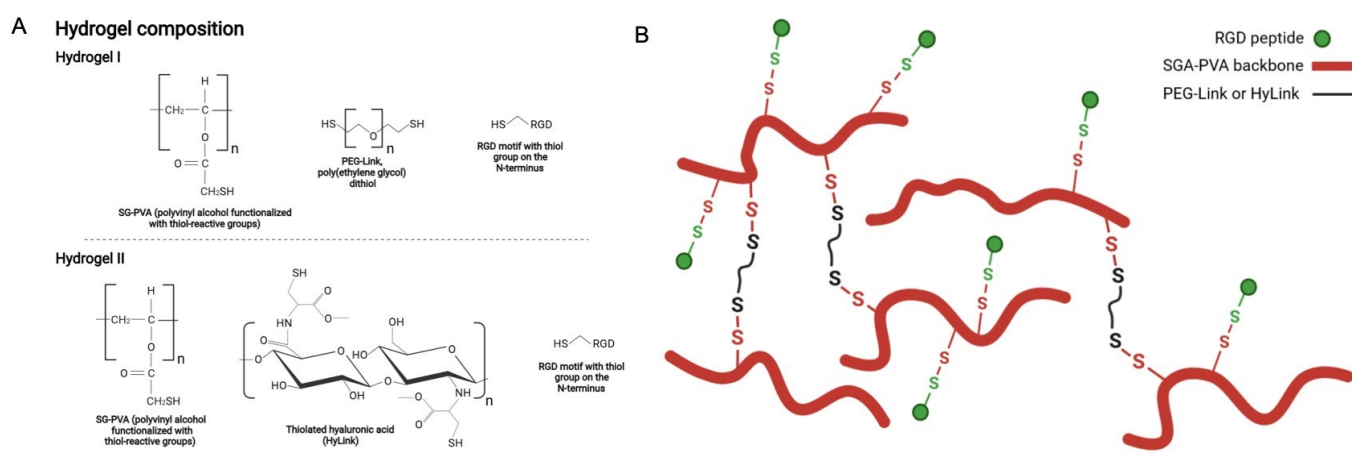
### Supplementary information

## Non-invasive analysis of pancreas organoids in synthetic hydrogels defines material-cell interactions and luminal composition

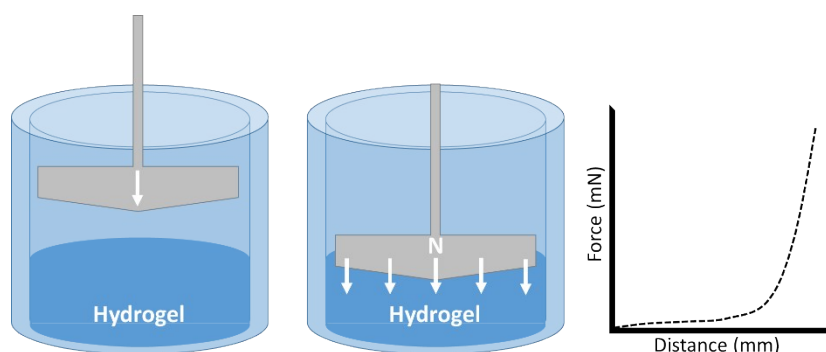
Nathalie Jung,<sup>a†</sup> Till Moreth,<sup>b†</sup> Ernst H. K. Stelzer,<sup>b</sup> Francesco Pampaloni<sup>b</sup> and Maike Windbergs<sup>a</sup>

<sup>a</sup> Institute of Pharmaceutical Technology and Buchmann Institute for Molecular Life Sciences, Goethe University, Frankfurt am Main, Germany.

<sup>b</sup> Buchmann Institute for Molecular Life Sciences, Goethe University, Frankfurt am Main, Germany.

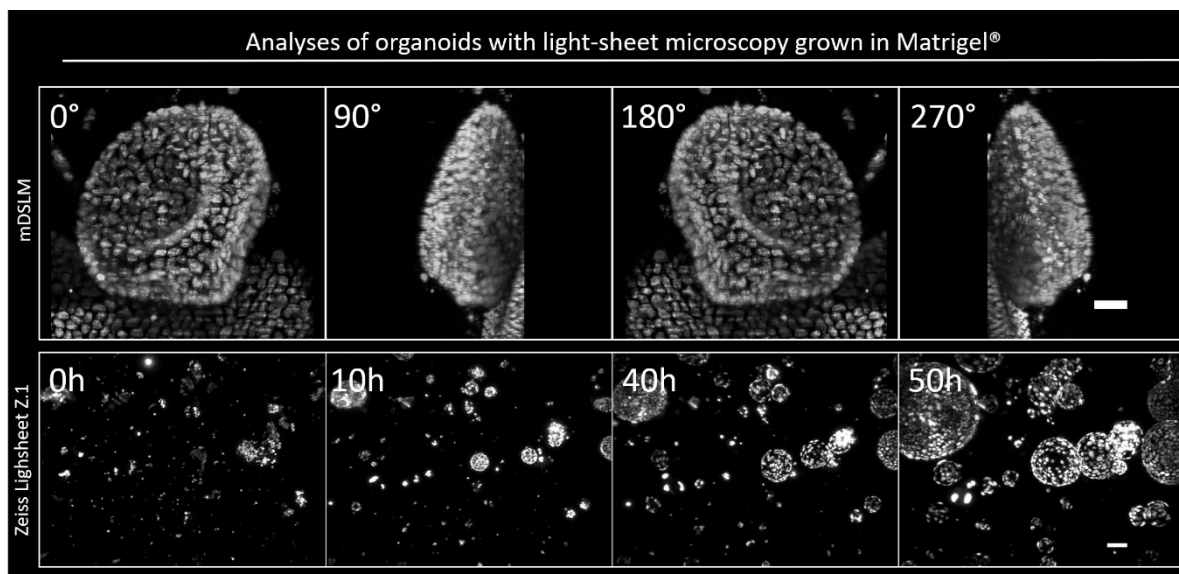


Supplemental Figure 1: Composition and structure of Hydrogel I and II. A: Structural formula of the components of both hydrogels. B: At a buffered pH of 7.5 an extensive cross link of the PVA backbone molecules is achieved through disulfide bonds with the cross-linking molecules (thiolated PEG and hyaluronic acid, respectively), resulting in the hydrogel formation. The RGD peptides are linked as well through disulfide bonds.



Supplemental Figure 2: Mechanical testing of hydrogels. Both hydrogels and Matrigel<sup>®</sup> were characterised regarding their mechanical properties and the stiffness of each gel by observing their behaviour during the application of pressure force. For this, 80  $\mu$ l of each gel were prepared as described above in a well of a 96 well plate and covered with 80  $\mu$ l

PBS after polymerisation. The gel was afterwards fixed in a single column force testing system (5940 Series, Instron, Germany) equipped with a static load cell (50 N capacity) where a stamp was lowered into the well with a speed of 2 mm/min while recording the applied pressure force. The test was programmed to stop at a force of 2 N which marks the contact of the stamp with the bottom of the well.



Supplemental Figure 3: State of the art approaches to investigate organoid growth; with digital scanned laser light-sheet microscope (mDSLIM) and conventional Static Light-sheet microscope (Carl Zeiss Lightsheet Z.1). The upper row shows a fixed pancreas organoid, stained with Dapi to illustrate the cell nuclei and imaged with a mDSLIM. Four different angles of one 3D-max-projected image stack are shown. The lower row shows organoids with transgenic labelled nuclei, developing over a time period of 50 hours inside the light sheet microscope Carl Zeiss Lightsheet Z.1. Cell Line: Mouse pancreatic organoids derived from a *rosa-nTnG* mouse (B6;129S6-Gt(ROSA)26Sortm1(CAG-tdTomato\*, -EGFP\*)Ees/J; Microscopes: mDSLIM, detection objective: N-Achroplan 10x/0.3; Zeiss Lightsheet Z.1, detection objective: W Plan-Apochromat 20x/1.0; Fluorophore: tdTomato, Dapi.

**Supplemental Movie 1:** Illustration of organoid formation in three different ECMs. From left to right, organoids growing for 120 hours in Matrigel, Hydrogel II (PVA-HA/RGD) and Hydrogel I (PVA-PEG/RGD) respectively. Organoids growing in Hydrogel II showing similar growth behaviour in comparison to Matrigel whereas in hydrogel I a delayed formation and a lower number of growing organoids are illustrated (arrows indicate growing organoids). Microscope: Zeiss CellObserver; Objective: Plan-Apochromat 5x/0.16, Stitched tiles per image: 9, Time of observation: 120 hours, recording-interval: 30 minutes.

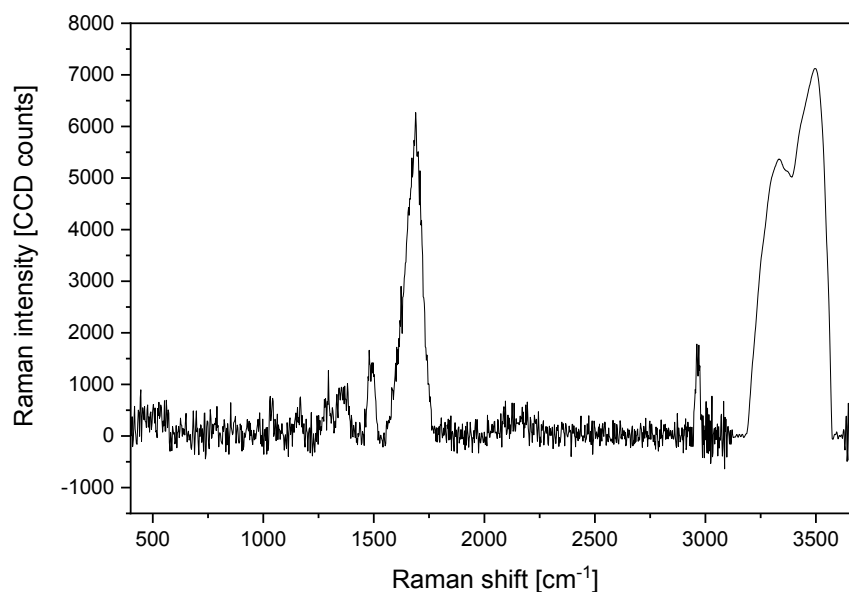
**Supplemental Movie 2:** Exemplary 3D-maximum projection of one pancreas organoid imaged with a monolithic light sheet-based fluorescence microscope (mDSLIM). The organoid is grown and fixed within an ultra-thin FEP-foil cuvette in Matrigel and stained with Dapi to visualise the cell nuclei. Microscopes: mDSLIM, objective: N-Achroplan 10x/0.30 fluorophore: Dapi, projected slices: 130.

**Supplemental Movie 3:** Time series of mouse pancreas organoids grown in an ultra-thin FEP-foil cuvette within the Zeiss Lightsheet microscope Z.1 for more than 50 hours. One complete sample holder, containing tenth of organoids, are imaged under close to nature conditions with a record interval of 30 minutes. Organoids expressing tdTomato in the nucleus. The image is build-up of 150 slices per time point as maximum-projections. The formation as well as the development of different sized organoids are illustrated. Cell line: Mouse pancreatic organoids derived from a *rosa-nTnG* mouse (B6;129S6-Gt(ROSA)26Sortm1(CAG-tdTomato\*, -EGFP\*)Ees/J; Microscopes: Zeiss Lightsheet Z.1; Objective: W Plan-Apochromat 20x/1.0; Fluorophore: tdTomato.

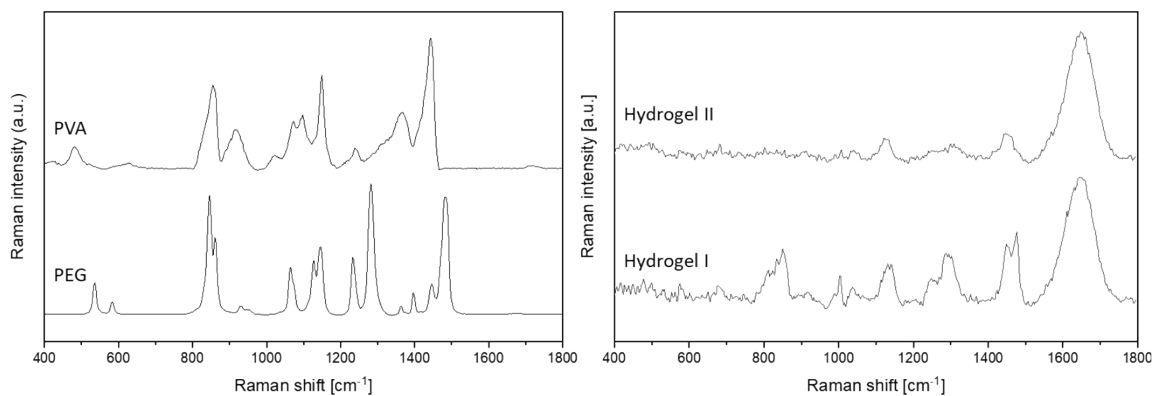
**Supplemental Movie 4:** Time series of a single mouse pancreas organoid imaged over 69 hours of development. After the formation process debris is collecting at the middle/bottom of the Organoid. During the growth of the organoid, single cells, presumably dead, are shed from the apical part of the structure into the lumen (indicated by black arrows). Dependent on the amount of dead cell and debris inside the organoid, the lipid and protein concentration detected via confocal Raman microscopy can provide information about the vitality of the organoid. Microscope: Zeiss CellObserver, objective: Plan-Apochromat 5x/0.16, Time of observation: 69 hours, record interval: 10 minutes.

Supplemental Table 1: Antibodies and Dyes

Primary Antibody	Dilution	Company	Reference	Dilution
<i>E-cadherin (DECMA-1)</i>	1:100	Abcam	ab11512	1 mg/ml
<i>Caspase-3 (active) Asp175</i>	1:200	Cell Signalling	#9661	-
<i>ZO-1 (C-19)</i>	1:100	Santa Cruz Biotechnology	sc-8146	0.2 mg/ml
<i>Sox9</i>	1:50	Merck Millipore	AB5535	1 mg/ml
<b>Secondary Antibody</b>				
<i>goat anti-rabbit IgG Alexa Fluor 488</i>	1:200	Thermo Fisher Scientific	A11008	2 mg/ml
<i>goat anti-rat IgG Alexa Fluor 633</i>	1:200	Thermo Fisher Scientific	A21094	2 mg/ml
<i>donkey anti-goat IgG Alexa Fluor 488</i>	1:200	Thermo Fisher Scientific	A11055	2 mg/ml
<i>goat anti-rabbit IgG Alexa Fluor 568</i>	1:200	Thermo Fisher Scientific	A11011	2 mg/ml
<b>Dyes</b>				
<i>Alexa Fluor® 546 Phalloidin</i>	1:400	Thermo Fisher Scientific	A22283	-
<i>Alexa Fluor® 647 Phalloidin</i>	1:400	Thermo Fisher Scientific	A22287	-
<i>Dapi (4',6-Diamidino-2-Phenylindole, Dilactate)</i>	1:400	Merck Millipore	124653	-



Supplemental Figure 4: Full Raman spectrum of the lumen of a mouse pancreas organoid grown in Matrigel for 7 days. The visualisation of the full Raman spectrum (400-3700  $\text{cm}^{-1}$ ) allows for the monitoring of not only the fingerprint region (400-1800  $\text{cm}^{-1}$ ) but for the high wave numbers beyond the “silent region” over 2800  $\text{cm}^{-1}$ . Here, Further information about the presence of protein (2939,8  $\text{cm}^{-1}$ ) and water (3280,5  $\text{cm}^{-1}$ ) can be gathered in order to perform the calculations of protein:water ratios shown in Figure 6.



Supplemental Figure 5: Raman spectra of Hydrogel I and Hydrogel II and reference Raman spectra of polyvinyl alcohol (PVA) and polyethylene glycol (PEG). Analysis of the two synthetic hydrogels were carried out with Raman spectroscopy. The gels display distinctly different peak patterns, representing their synthetic composition: Hydrogel I contains Raman peaks associated to polyvinyl alcohol (PVA, at 854 and 1443  $\text{cm}^{-1}$ ) and polyethylene glycol (PEG, at 844, 1129, 1282 and 1484  $\text{cm}^{-1}$ ), as well as Raman peaks attributed to peptide derived molecular bonds (998, 1440, 1644  $\text{cm}^{-1}$ ). The Raman spectrum of Hydrogel II however is dominated by Raman peaks associated to the added peptides while the concentration of PVA and hyaluronic acid might be too low to contribute significantly to its Raman spectrum.